



1 **Characteristics and mixing state of amine-containing**
2 **particles at a rural site in the Pearl River Delta, China.**

3
4 Chunlei Cheng^{1,2}, Zuzhao Huang³, Chak K. Chan⁴, Yangxi Chu⁴, Mei Li^{1,2*}, Tao
5 Zhang⁵, Yubo Ou⁵, Duohong Chen⁵, Peng Cheng^{1,2}, Lei Li^{1,2}, Wei Gao^{1,2}, Zhengxu
6 Huang^{1,2}, Bo Huang^{1,2,6}, Zhong Fu⁶, Zhen Zhou^{1,2*}

7
8 ¹Institute of Mass Spectrometer and Atmospheric Environment, Jinan University, Guangzhou 510632,
9 China

10 ²Guangdong Provincial Engineering Research Center for on-line source apportionment system of air po
11 llution, Guangzhou 510632, China

12 ³Guangzhou Environmental Technology Assessment Center, Guangzhou 510045, China

13 ⁴School of Energy and Environment, City University of Hong Kong, Hong Kong, China

14 ⁵State Environmental Protection Key Laboratory of Regional Air Quality Monitoring, Guangdong
15 Environmental Monitoring Center, Guangzhou 510308, China

16 ⁶Guangzhou Hexin Analytical Instrument Limited Company, Guangzhou 510530, China

17

18

19 **Correspondence to:* Mei Li (limei2007@163.com) and Zhen Zhou (zhouzhen@gig.ac.cn)

20 Tel: 86-20-85225991, Fax: 86-20-85225991

21

22

23

24

25

26

27

28

29

30

31

32

33

34

35

36

37

38

39

40

41

42



43 **Abstract.** Particulate amines play an important role for the particle acidity and
44 hygroscopicity and also contribute to secondary organic aerosol mass. We investigated
45 the sources and mixing states of particulate amines using a single-particle aerosol
46 mass spectrometer (SPAMS) during summer and winter 2014 at a rural site in the
47 Pearl River Delta, China. Amine-containing particles accounted for 12.8 % and 9.2 %
48 of the total detected individual particles in summer and winter, respectively.
49 Amine-containing particles were classified into three types: elemental and organic
50 carbon (ECOC), biomass burning (BB), and nitrate-rich. ECOC amine-containing
51 particles were the most abundant, constituting 67.2 % and 74.8 % of amine particles
52 in summer and winter, respectively. Both ECOC and BB type amine-containing
53 particles contained abundant carbonaceous and carbon-nitrogen species, as well as
54 sulfate and nitrate, in summer and winter. The nitrate-rich amine-containing particles
55 were mixed with abundant sea-salt markers in summer, indicating a possible
56 association between the amine emission source and marine phytoplankton. In summer,
57 only 6.7 % of the total amine-containing particles were found to be mixed with
58 ammonium, while in winter this percentage increased to 55 %. The ammonium-poor
59 state of amine-containing particles in summer may have been caused by the
60 displacement of particle-phase ammonium by amine uptake, which was more efficient
61 in summer at higher ambient RH (72 ± 13 %) than in winter (63 ± 11 %). In
62 ECOC-type amine-containing particles, the time series of the amine peak area and the
63 sum of the nitrate and sulfate peak areas were similar in both summer and winter,
64 suggesting the formation of aminium sulfate and nitrate salts. The particle acidity of
65 ECOC-type amine-containing particles was represented by the relative acidity ratio
66 (R_a), which was defined as the ratio of the total sulfate and nitrate peak areas to the
67 ammonium peak area. The R_a decreased from 348 ± 335 and 28 ± 14 to 10 ± 5 and $9 \pm$
68 2 in summer and winter, respectively, after including amines along with the
69 ammonium in the acidity calculation, suggesting that it is reasonable to consider
70 amines when estimating particle acidity. Based on the influence of amines on
71 particulate ammonium and particle acidity, particulate amines could have an impact
72 on the newly found ‘missing’ source of sulfate produced from the oxidation of SO_2 by



73 NO₂ with NH₃ neutralization during haze episodes under high ambient relative
74 humidity in northern China.

75 **Keywords:** Amine; Single particles; Mixing state; Aminium salts; Particle acidity;
76 SPAMS.

77 **1 Introduction**

78 Amines, a group of nitrogen-containing organic compounds, are ubiquitous in
79 the atmospheric gas and particle phases (Ge et al., 2011a). A variety of low molecular
80 weight (LMW) aliphatic amines have been detected in emissions from anthropogenic
81 and natural sources, including animal husbandry, biomass burning, industrial
82 emissions, vehicle exhaust, and marine sources (Rogge et al., 1994; Rappert and
83 Muller, 2005; Calderon et al., 2007; Ngwabie et al., 2007; Ge et al., 2011a). LMW
84 aliphatic amines have gas-phase concentrations two orders of magnitude lower than
85 that of ammonia (NH₃) (Sorooshian et al., 2008), but are more alkaline than NH₃ (Ge
86 et al., 2011b). Due to their strong basicity and water solubility, LMW amines can
87 undergo acid-base reactions with sulfuric and nitric acid to form aminium salts
88 (Angelino et al., 2001; Sorooshian et al., 2007; Pratt et al., 2009), which has been
89 found to enhance new particle formation beyond the amounts produced from reactions
90 between acids and NH₃ alone (Kurten et al., 2008; Berndt et al., 2010; Place et al.,
91 2010; Wang et al., 2010). In addition, once partitioned into the particle phase, these
92 LMW aliphatic amines can enhance aerosol particle hygroscopicity (Chu et al., 2015;
93 Sauerwein et al., 2015). Furthermore, amines can be oxidized by OH radicals, NO₃
94 radicals, and O₃ in the atmosphere to form semi-volatile and non-volatile compounds,
95 some of which are highly toxic (Lee and Wexler, 2013), and which contribute to
96 secondary organic aerosol (SOA) mass (Murphy et al., 2007; Malloy et al., 2009).

97 The mass concentration and temporal distribution of LMW aliphatic amines in
98 aerosols have been studied extensively in a variety of environments, and LMW
99 aliphatic amines account for 2–12 % of organic mass (Day et al., 2009; Gilardoni et
100 al., 2009; Liu et al., 2009; Russell et al., 2009; Williams et al., 2010). In recent years,
101 real-time single particle mass spectrometry has been used to measure the size and



102 chemical composition of individual amine-containing particles with high time
103 resolution. The mixing state and single-particle characteristics of amines have been
104 investigated in laboratory and field environments (Moffet et al., 2008; Silva et al.,
105 2008; Pratt et al., 2009; Huang et al., 2012; Zhang et al., 2012). Pratt et al. (2009)
106 studied seasonal differences in aminium and ammonium salts on a single-particle
107 basis using an aerosol time-of-flight mass spectrometer (ATOFMS) coupled with a
108 thermodenuder and reported that the gas-to-particle partitioning of amines is
109 dependent on particle acidity. Healy et al. (2015) investigated the temporal
110 distributions of alkylamines at five European sites, and found that alkylamines were
111 internally mixed with both sulfate and nitrate, which suggests that the formation of
112 aminium salts was important at all sites. Huang et al. (2012) determined the mixing
113 state of amine-containing particles in Shanghai and found higher number
114 concentrations of amine-containing particles in winter than in summer, which they
115 attributed to effective acid-base reactions between sulfuric acid and amines under
116 low-temperature, high-RH conditions. Zhang et al. (2012) measured
117 trimethylamine-containing particles in Guangzhou and found preferential
118 trimethylamine gas-to-particle partitioning during fog events. These field observations
119 emphasize the important role of acid-base reactions in the partitioning of amines from
120 the gas phase to the particle phase. Recent laboratory studies have revealed that the
121 exchange between amine gases and particulate NH_3 and/or ammonium also
122 contributes substantially to amine content and results in a depletion of NH_3 and/or
123 ammonium in the particle phase (Lloyd et al., 2009; Bzdek et al., 2010; Qiu et al.,
124 2011; Liu et al., 2012; Chan and Chan, 2013; Chu and Chan, 2016, 2017; Sauerwein
125 and Chan, 2017); however, the significance of such exchange reactions in the ambient
126 environment has not been fully explored. Therefore, the influence of ammonia and
127 particle acidity on the distribution of amines in the particle phase should be studied
128 comprehensively through field measurements.

129 The aim of this study was to investigate the mixing state of a series of LMW
130 aliphatic amines with sulfate, nitrate, and ammonium in individual particles using a
131 single-particle aerosol mass spectrometer (SPAMS) at a rural site in the Pearl River



132 Delta, China. In order to explore amine origins and gas-to-particle partitioning
133 processes, amine-containing particles from both summer and winter were classified
134 into three types based on mass spectral patterns. The aminium sulfate and nitrate salt
135 formation processes and internal mixing state with ammonium were used to deduce
136 the relationship between amines and ammonium in the particle phase and the
137 influence of amines on particle acidity.

138 **2 Methods**

139 **2.1 Aerosol sampling**

140 Ambient single particles were collected and analyzed using a SPAMS at the
141 Guangdong Atmospheric Supersite (22.73° N, 112.93° E), a rural site in Heshan City
142 in the Pearl River Delta (PRD), China (Figure S1). The sampling site is surrounded by
143 villages and experiences little influence from local industrial emissions (Cheng et al.,
144 2017). The SPAMS was installed at the top of the main building, and aerosols were
145 introduced to the SPAMS through a 2.5 m copper tube. SPAMS sampling was
146 conducted continuously from 18 July to 1 August 2014 and from 27 January to 8
147 February 2015; several hours of data are missing due to technical maintenance.
148 During the sampling period, hourly O₃ concentrations were measured using an O₃
149 analyzer (model 49i, Thermo Scientific). Meteorological data, including temperature,
150 relative humidity, wind speed, and wind direction, were also measured during SPAMS
151 sampling.

152 **2.2 SPAMS**

153 SPAMS was designed by the Guangzhou Hexin Analytical Company based on
154 preexisting ATOFMS principles (Prather et al., 1994; Noble and Prather, 1996). The
155 setup and design of the SPAMS has been detailed previously (Li et al., 2011). Briefly,
156 single particles are sampled through an 80 μm critical orifice into the aerodynamic
157 lens at a flow rate of 75 ml min⁻¹. Then, the particles pass consecutively through two
158 laser beams (diode Nd:YAG, 532 nm) spaced 6 cm apart, and the aerodynamic
159 diameter of the single particle is calculated using the particle flight time and velocity
160 between the two laser beams. The single particle velocity is also used to calculate the



161 precise time at which to fire the desorption and ionization laser (Nd:YAG laser,
162 266nm), which is positioned 12 cm downstream from the second laser beam. After
163 ionization, the positive and negative ions are detected by a Z-shaped bipolar
164 time-of-flight mass spectrometer. In this work, the ionization laser pulse energy was
165 0.6 mJ and the power density was $1.06 \times 10^8 \text{ W cm}^{-2}$ throughout the campaign. The
166 size range of single particles detected by SPAMS ranged from 0.2 to 2 μm , calibrated
167 with standard polystyrene latex spheres (Nanosphere size standards, Duke Scientific
168 Corp., Palo Alto) of 0.22–2.0 μm diameter before and after the campaign (Cheng et al.,
169 2017).

170 2.3 Data analysis

171 Particle size and chemical composition were obtained via SPAMS mass spectral
172 analysis using the Computational Continuation Core (COCO; version 3.0) toolkit in
173 Matlab. Based on previous studies using ATOFMS and SPAMS instruments
174 (Angelino et al., 2001; Huang et al., 2012; Zhang et al., 2012; Healy et al., 2015),
175 amine-containing particles were characterized by ionic markers, including m/z 46
176 $[(\text{CH}_3)_2\text{NH}_2]^+$, 59 $[(\text{CH}_3)_3\text{N}]^+$, 74 $[(\text{C}_2\text{H}_5)_2\text{NH}_2]^+$, 86 $[(\text{C}_2\text{H}_5)_2\text{NCH}_2]^+$ or
177 $[\text{C}_3\text{H}_7\text{NHC}_2\text{H}_4]^+$, 101 $[(\text{C}_2\text{H}_5)_3\text{N}]^+$, 102 $[(\text{C}_3\text{H}_7)_2\text{NH}_2]^+$, 114 $[(\text{C}_3\text{H}_7)_2\text{NCH}_2]^+$, and 143
178 $[(\text{C}_3\text{H}_7)_3\text{N}]^+$, which correspond to dimethylamine (DMA), trimethylamine (TMA),
179 diethylamine (DEA), triethylamine (TEA), dipropylamine (DPA), and tripropylamine
180 (TPA). In this work, a particle was identified as amine-containing if it contained any
181 of the marker ions listed above with a relative peak area (defined as the percentage
182 contribution of the target ion peak area to the sum of all ion peak areas) greater than
183 1 %. According to this criterion, 66331 and 70648 amine-containing particles were
184 identified in summer and winter, respectively, which accounted for 12.8 % and 9.2 %
185 of the total detected particles. These number fractions are consistent with previously
186 reported observations in the PRD (Zhang et al., 2012). However, due to the absence of
187 fog events during the campaign, no dramatic increases in amine-containing particles
188 associated with high RH conditions (RH > 90 %) were observed. Amine-containing
189 particles were subsequently clustered using the adaptive resonance theory (ART-2a)
190 neural network algorithm with a vigilance factor of 0.75, a learning rate of 0.05, and a



191 maximum of 20 iterations.

192 The amine-containing particles were classified into three types: elemental and
193 organic carbon (ECOC), biomass burning (BB), and nitrate-rich. The ion markers and
194 selective criterion for these three particle types are as follows (Table S1): (1)
195 ECOC-type particles contain abundant carbon clusters of $m/zs \pm 12 [C]^{+/-}$, $\pm 24 [C_2]^{+/-}$,
196 $\pm 36 [C_3]^{+/-}$, and hydrocarbon clusters at $m/zs 37 [C_3H]^+$ and $43 [C_3H_7]^+/[C_2H_3O]^+$
197 with relative peak areas higher than 0.5 %; (2) BB-type particles consist of any
198 remaining particles containing abundant signal at $m/z 39 [K]^+$ (relative peak area >
199 30 %) and $m/zs -59 [C_2H_3O_2]^-$ and $-73 [C_3H_5O_2]^-$ (relative area of both peaks > 0.5 %);
200 (3) any remaining particles containing abundant signal at $m/zs -46 [NO_2]^-$ and -62
201 $[NO_3]^-$ with relative peak areas higher than 10% are classified as nitrate-rich. The
202 above classification protocol for amine-containing particles has been used in other
203 studies (Bi et al., 2011; Pratt et al., 2011; Zhang et al., 2013). These three types of
204 amine-containing particles constitute 93.5 % and 94.8 % of the total amine-containing
205 particles in summer and winter, respectively.

206 3 Results and Discussion

207 3.1 Seasonal variation of amine-containing particles

208 Meteorological conditions, namely wind speed and wind direction, are shown
209 during the sampling period in Figure 1. In summer, high amine-containing particle
210 number concentrations were associated with southwesterly and southeasterly winds at
211 speeds of 3–5 $m s^{-1}$, suggesting that the majority of amine-containing particles came
212 from regional transport. However, in winter, large amounts of amine-containing
213 particles were associated with northwesterly winds at speeds of 0.5–2 $m s^{-1}$, indicating
214 that amine-containing particles were related primarily with local emissions, such as
215 animal husbandry, biomass burning, and vehicle exhaust. Anthropogenic emissions
216 from Foshan and Guangzhou may also have contributed, as the sampling site is only
217 40 km and 56 km from these cities, respectively (Figure S1).

218 Temporal variations in amine-containing particles and meteorological data (i.e.,
219 RH, temperature, wind speed, and wind direction) are shown in Figure 2.



220 Amine-containing particles showed different trends in summer and winter, and high
221 concentrations of amine-containing particles were found from 22 to 24 July (in
222 summer) and from 5 to 8 February (in winter). The amine-containing particle count
223 observed in summer (66 331) was lower than it observed in winter (70 648), but the
224 abundance of amine-containing particles relative to the total particle count was higher
225 in summer (12.8 %) than in winter (9.2 %). Amine-containing particles had similar
226 diurnal patterns in summer and winter (Figure 3), and both showed higher count at
227 night; the small increase from 6:00 to 9:00 LST throughout the campaign may have
228 been due to local emissions from vehicle exhaust (Cadle and Mulawa, 1980). Many
229 field studies have revealed a strong correlation between relative humidity (RH) and
230 particulate amines, suggesting that high RH in fog events is favorable for the
231 gas-to-particle partitioning of amines (Jeong et al., 2011; Rehbein et al., 2011; Huang
232 et al., 2012; Zhang et al., 2012). In this work, the correlation between
233 amine-containing particle count and ambient RH was not obvious in either summer or
234 winter (Figure S2). Other factors, such as particle acidity, may have contributed to the
235 acid-base reactions that formed the aminium salts (Murphy et al., 2007; Kurten et al.,
236 2008; Silva et al., 2008).

237 **3.2 Mass spectra of amine-containing particles**

238 Amine-containing particles were categorized as ECOC, BB, and nitrate-rich both
239 in summer and winter. ECOC amine-containing particles were dominant, accounting
240 for 67.2 % and 74.8 % of particle count in summer and winter, respectively (Table 1).
241 ECOC particles exhibited variations similar to those in total amine-containing
242 particles in both summer and winter. Nitrate-rich particles were the second most
243 abundant in summer, during which time they accounted for 13.4 % of total
244 amine-containing particles, while BB particles were the second most abundant in
245 winter, accounting for 16.3 % of total amine-containing particles. Nitrate-rich
246 particles were three times more abundant in summer than in winter, suggesting the
247 existence of aminium nitrate salts in summer.

248 The average mass spectra of ECOC, BB, and nitrate-rich amine-containing
249 particles in summer and winter are shown in Figure 4. The ECOC amine-containing



250 particles in both summer and winter were characterized by high fractions of 39 [K]⁺;
251 carbonaceous marker ions, including *m/z*s 27 [C₂H₃]⁺, 29 [C₂H₅]⁺, 36 [C₃]⁺, 37 [C₃H]⁺,
252 43 [C₂H₃O]⁺, 48 [C₄]⁺, 51 [C₄H₃]⁺, 53 [C₄H₅]⁺, 60 [C₅]⁺, 63 [C₅H₃]⁺, 65 [C₅H₅]⁺, and
253 77 [C₆H₅]⁺; and amine fragment ions at *m/z*s 46 [(CH₃)₂NH₂]⁺, 59[(CH₃)₃N]⁺, 74
254 [(C₂H₅)₂NH₂]⁺, and 86 [(C₂H₅)₂NCH₂]⁺/[C₃H₇NHC₂H₄]⁺ in the positive mass
255 spectrum. The ECOC particle negative mass spectrum was characterized by strong
256 carbon-nitrogen fragment signals at *m/z*s -26 [CN]⁻ and -42 [CNO]⁻, as well as
257 abundant secondary ions at *m/z*s -46 [NO₂]⁻, -62 [NO₃]⁻, -80 [SO₃]⁻, and -97 [HSO₄]⁻
258 in both summer and winter. In many field studies, aged carbonaceous particles always
259 contain abundant secondary sulfate, nitrate, and ammonium ions. Interestingly, in this
260 work, the ammonium signal (*m/z* 18 [NH₄]⁺) was not found in ECOC
261 amine-containing particles in summer, and only a very small ammonium peak was
262 detected in winter. The low ammonium signal in ECOC amine-containing particles
263 may have been due to the exchange of particulate ammonium for gas-phase amines
264 (Lloyd et al., 2009; Qiu et al., 2011; Chan and Chan, 2012; Chan and Chan, 2013;
265 Chu and Chan, 2016, 2017; Sauerwein and Chan, 2017). In both summer and winter,
266 the mass spectra of BB amine-containing particles showed carbonaceous markers and
267 secondary ions similar to those found in ECOC amine-containing particles, with
268 additional distinct ion peaks at *m/z* 23 [Na]⁺ and BB markers at *m/z*s -59 [C₂H₃O₂]⁻,
269 -71 [C₃H₃O₂]⁻, and -73 [C₃H₅O₂]⁻. No ammonium was found in BB amine-containing
270 particles in either summer or winter, likely because of exchange reactions similar to
271 those inferred in the ECOC amine-containing particles (see Section 3.3).

272 The nitrate-rich amine-containing particles exhibited spectral features different
273 from those observed in the ECOC and BB spectra. Only a few carbonaceous
274 fragments were observed. In summer, the nitrate-rich amine-containing particles
275 contained abundant sea-salt markers such as *m/z*s 23 [Na]⁺, 62 [Na₂O]⁺, and
276 63[Na₂OH]⁺ in the positive mass spectrum and *m/z*s -93 [NaCl₂]⁻ and -147
277 [Na(NO₃)₂]⁻ in the negative mass spectrum. Chloride signal was not detected due to
278 the depletion of chloride and enrichment of nitrate in the sea-salt particle aging
279 process (Gard et al., 1998). In summer, 48-h backward trajectories showed that 60 %



280 of air masses arose from marine areas (Figure S3) and were partly associated with
281 marine aerosols. A small peak of m/z 46 $[(\text{CH}_3)_2\text{NH}_2]^+$ was found in the nitrate-rich
282 amine-containing particle spectra in summer, which likely arose from DMA produced
283 by marine phytoplankton (Facchini et al., 2008). The backward trajectories and mass
284 spectra of the nitrate-rich particles indicate that marine sources may contribute to the
285 amine distribution in the PRD region during summer, although the amine-containing
286 particles appeared to have been aged during transportation. In winter, air masses were
287 transported largely from urban areas like Guangzhou and Foshan (Figure S3) and
288 brought more anthropogenic pollutants to the sampling site. Hence, the sea-salt
289 markers at m/z s -93 $[\text{NaCl}_2]^-$ and -147 $[\text{Na}(\text{NO}_3)_2]^-$ were not observed in the winter
290 negative mass spectrum. Instead, the m/z 56 $[\text{Fe}]^+$ ion was identified, and, because no
291 dust source marker ion signals (such as Ca^+ , CaO^+ , and SiO_3^-) were found, we
292 speculate that iron arose mainly from industrial emissions. The nitrate-rich
293 amine-containing particles may have resulted from direct industrial emissions or
294 reactions between gaseous amines and particles from industrial emissions. Lastly, the
295 observed nitric acid signal (m/z -125 $[\text{HNO}_3\text{NO}_3]^-$) indicated strong particle acidity in
296 the nitrate-rich amine-containing particles in winter.

297 Size-resolved number distributions are shown in Figure 5 for the three types of
298 amine-containing particles. Both ECOC and BB amine-containing particles exhibited
299 unimodal distributions in the submicron mode and had a broad distribution from 0.4
300 to 1.0 μm in both summer and winter, which may have resulted from amine
301 condensation on and reaction with fine mode particles from anthropogenic emissions.
302 Interestingly, in summer, 37 % of the nitrate-rich amine-containing particles were
303 submicron in size, while 63 % were supermicron; this is reasonable, as the majority of
304 nitrate-rich amine-containing particles were associated with sea-salt particles from
305 marine sources. Healy et al. (2015) also reported large amounts of supermicron
306 amine-containing particles internally mixed with sea-salt particles on the island of
307 Corsica, France.

308 3.3 Mixing states and formation processes of amine-containing particles

309 To investigate the seasonal mixing states of amines with sulfate, nitrate, and



310 ammonium (SNA), the relative abundances of SNA-containing amine particles are
311 shown in Figure 6. The color scale represents the percentage contribution of
312 SNA-containing amine particles to total amine particles. ECOC and BB
313 amine-containing particles were both found to be internally mixed with sulfate
314 throughout the sampling period. Only a small percentage of nitrate-rich
315 amine-containing particles were mixed with sulfate during summer, but this
316 percentage increased to 53 % during winter. Amine particles containing nitrate
317 accounted for 39 % and 59 % of the ECOC and BB particles in summer, respectively,
318 and 68 % and 79 % in winter. The internal mixing state of sulfate and nitrate with
319 amines in single particles suggests the possible formation of aminium sulfate and
320 nitrate salts. Only 6.7 % of the total amine-containing particles contained ammonium
321 in summer, while percentage increased dramatically to 55 % in winter, indicating an
322 ammonium-poor state in summer and an ammonium-rich state in winter. The
323 particle-phase mixing states of ammonium and amines may be influenced by seasonal
324 changes in ambient meteorological conditions (such as RH and temperature) and
325 chemical processes involving particle acidity and/or ammonium–amine exchange
326 reactions. Since no correlation was observed between RH and amine-containing
327 particles during the sampling period (Figure S2), seasonal variations in temperature
328 may have had an impact on the mixing states of ammonium and amines in the particle
329 phase. The temperature dropped by 15 °C between summer (29 ± 3.0 °C) and winter
330 (14 ± 3.1 °C). Although lower temperatures favor the partitioning of both gaseous
331 ammonia and amines into the particulate phase (Huang et al., 2012), no obvious
332 enhancement was found in the amine-containing particle count in winter (Table 1);
333 this suggests that the increase in ammonium-containing amine particles was caused by
334 other factors, such as particle acidity and ammonium–amine exchange.

335 Strong sulfate and nitrate signals were detected in the amine-containing particle
336 mass spectra in both summer and winter, suggesting that gas-to-particle amine
337 partitioning may have been correlated with particle acidity. Due to the dominance of
338 ECOC amine-containing particles throughout the sampling period, the temporal
339 variations in the peak areas of amines, ammonium, and the sum of sulfate and nitrate



340 in ECOC particles are shown in Figure 7. The peak areas of amines and the sum of
341 nitrate and sulfate in ECOC particles varied similarly in summer and winter,
342 indicating the formation of aminium salts. Little ammonium was found in the
343 amine-containing particles in summer, while ammonium exhibited peak areas
344 comparable to those for amines in winter and temporal trends of ammonium and
345 amines were also similar. The sum of the sulfate and nitrate peak areas had a higher
346 increase rate than the amine peak area from 6 to 8 February, which may have been
347 caused by an increase in ammonium during this period.

348 Particle acidity affects the partitioning of gaseous ammonia and amines into the
349 particle phase and may be an important factor in the seasonal differences in
350 ammonium in amine-containing particles. In this study, the amine-containing particle
351 acidity is represented by the relative acidity ratio (R_a), which is defined as the ratio of
352 the sum of the sulfate and nitrate peak areas divided by the ammonium peak area
353 (Denkenberger et al., 2007; Pratt et al., 2009; Cheng et al., 2017). The ECOC particle
354 R_a was 348 ± 335 in summer and 28 ± 14 in winter (Figure 7), indicating that the
355 amine-containing particles were more acidic in summer than in winter. Although high
356 acidity is favorable for gaseous ammonia partitioning, extremely low ammonium peak
357 areas were found for the amine-containing particles in summer (Figure 7), which may
358 have been caused by the displacement of ammonium in the particle phase by amines
359 to form aminium sulfate and nitrate salts; this displacement depends on RH and the
360 phase of the ammonium salts (Chan and Chan, 2013; Chu and Chan, 2016). The
361 ambient RH in summer (72 ± 13 %) was higher than that in winter (63 ± 11 %). Thus,
362 it is feasible that particles contained more water and a larger fraction of aqueous
363 ammonium salts in summer than in winter, which facilitated the displacement of
364 ammonium by amines, decreasing the ammonium concentration in the particle phase.
365 Particle-phase organics other than amines and aminium salts also affect amine–
366 ammonia exchange (Chu and Chan, 2016, 2017). However, because the SPAMS alone
367 cannot provide quantitative data on particle-phase organics, this issue will be
368 discussed in a subsequent study.

369 The strong correlation between the amine peak areas and the sulfate and nitrate



370 peak areas may indicate a feedback between amines and particle acidity. If one
371 includes amines in the R_a calculation, the new R_a' values (redefined as the ratio of the
372 sum of the sulfate and nitrate peak areas to the sum of the ammonium and amine peak
373 areas) decrease to 10 ± 5 and 9 ± 2 in summer and winter, respectively, which are 30
374 and 3 times lower than R_a values excluding amines. In addition, the presence of
375 ammonium salts affects the water activities and osmotic coefficients of aqueous
376 solutions, which may influence the calculation of particle acidity using aerosol
377 thermodynamic models (Sauerwein et al., 2015). Furthermore, it should be noted that
378 the measured pH of bulk ambient aerosols may not be representative of the actual
379 single particle acidity. Hence, the mixing state of aerosols should be considered in
380 order to comprehensively estimate the aerosol pH (Pratt et al., 2009).

381 Several recent studies have reported a ‘missing’ source of sulfate produced from
382 the oxidation of SO_2 by NO_2 during haze episodes with high ambient relative
383 humidity in northern China, and the neutralization of particulate ammonium is a key
384 factor in this formation mechanism (Cheng et al., 2016; Wang et al., 2016). Our study
385 reveals that amines significantly influence particulate ammonium and particle acidity;
386 thus, particulate amines could also impact this sulfate formation process during haze
387 episodes. In order to discuss the potential role of amines in this sulfate formation
388 pathway, real-time concentrations of amines, ammonium, sulfate, nitrate, and their
389 precursors must be available.

390 **4 Summary and Conclusions**

391 Amine-containing particles were investigated using a single particle aerosol mass
392 spectrometer from 18 July to 1 August 2014, and from 27 January to 8 February 2015
393 in Heshan, China. Amine-containing particles accounted for 12.8 % and 9.2 % of the
394 total detected single particles in summer and winter, respectively; both seasons were
395 dominated by ECOC-type amine particles at percentages of 67.2 % and 74.8 %,
396 respectively. The ECOC and BB amine-containing particles showed strong
397 carbonaceous ion, carbon-nitrogen ion, sulfate, and nitrate signals in summer and
398 winter. However, little ammonium was found in these amine-containing particles in



399 summer, and small ammonium peaks were observed in winter. In summer, the
400 nitrate-rich amine-containing particles were mixed with abundant sea-salt markers,
401 indicating an association between amines and marine phytoplankton emissions. In
402 ECOC amine-containing particles, the amine peak area and the sum of the nitrate and
403 sulfate peak areas varied similarly in summer and winter, suggesting the formation of
404 aminium sulfate and nitrate salts. An analysis of the relative acidity ratio indicated
405 that ECOC amine-containing particles were more acidic in summer than in winter.
406 However, in summer, only 6.7 % of the amine-containing particles contained
407 ammonium; this percentage increased dramatically to 55 % in winter. The
408 ammonium-poor state of the amine-containing particles in summer may have been
409 caused by the displacement of ammonium in the particle phase by amines to form
410 aminium sulfate and nitrate salts. The significant influence of amines on the ratio of
411 sulfate and nitrate to ammonium suggests that amines should be taken into
412 consideration when estimating particle acidity.

413

414 **Author contributions:** Chunlei Cheng and Mei Li designed the experiments. Tao
415 Zhang, Yubo Ou and Duohong Chen carried them out. Chunlei Cheng prepared the
416 manuscript with contributions from all co-authors.

417

418 **Competing interests:** Bo Huang and Zhong Fu are both employees at Guangzhou
419 Hexin Analytical Instrument Limited Company.

420

421 **Acknowledgements:** This work was financially supported by the National Natural
422 Science Foundation of China (Grant No.21607056), NSFC of Guangdong Province
423 (Grant Nos. 2017A030310180, 2015A030313339), National Key Technology R&D
424 Program (Grant No. 2014BAC21B01), Guangdong Province Public Interest Research
425 and Capacity Building Special Fund (Grant No. 2014B020216005), Fundamental
426 Research Funds for the Central Universities (Grant No. 21617455), National Key
427 Research and Development Program of China (Grant No. 2016YFC0208503), and
428 Pearl River Nova Program of Guangzhou (No. 201506010013). Chak K. Chan would



429 like to acknowledge funding support from the General Fund of National Natural
430 Science Foundation of China (Grant No. 41675117). The authors acknowledge
431 sampling support from the Guangdong Atmospheric Supersite. Helpful comments and
432 revisions from Anthony S. Wexler and Misha I.S. Boehm are acknowledged as well.

433 **References**

- 434 Angelino, S., Suess, D. T., and Prather, K. A.: Formation of aerosol particles from
435 reactions of secondary and tertiary alkylamines: Characterization by aerosol
436 time-of-flight mass spectrometry, *Environ Sci Technol*, 35, 3130-3138, Doi
437 10.1021/Es0015444, 2001.
- 438 Berndt, T., Stratmann, F., Sipila, M., Vanhanen, J., Petaja, T., Mikkila, J., Gruner, A.,
439 Spindler, G., Mauldin, R. L., Curtius, J., Kulmala, M., and Heintzenberg, J.:
440 Laboratory study on new particle formation from the reaction OH + SO₂:
441 influence of experimental conditions, H₂O vapour, NH₃ and the amine
442 tert-butylamine on the overall process, *Atmos Chem Phys*, 10, 7101-7116,
443 10.5194/acp-10-7101-2010, 2010.
- 444 Bi, X., Zhang, G., Li, L., Wang, X., Li, M., Sheng, G., Fu, J., and Zhou, Z.: Mixing
445 state of biomass burning particles by single particle aerosol mass spectrometer in
446 the urban area of PRD, China, *Atmos Environ*, 45, 3447-3453, 2011.
- 447 Bzdek, B., Ridge, D., and Johnston, M.: Amine exchange into ammonium bisulfate
448 and ammonium nitrate nuclei, *Atmos Chem Phys*, 10, 3495-3503, 2010.
- 449 Cadle, S. H., and Mulawa, P. A.: Low-molecular-weight aliphatic amines in exhaust
450 from catalyst-equipped cars, *Environ Sci Technol*, 14, 718-723, 1980.
- 451 Calderon, S. M., Poor, N. D., and Campbell, S. W.: Estimation of the particle and gas
452 scavenging contributions to wet deposition of organic nitrogen, *Atmos Environ*,
453 41, 4281-4290, 10.1016/j.atmosenv.2006.06.067, 2007.
- 454 Chan, L. P., and Chan, C. K.: Displacement of ammonium from aerosol particles by
455 uptake of triethylamine, *Aerosol Sci Tech*, 46, 236-247, 2012.
- 456 Chan, L. P., and Chan, C. K.: Role of the Aerosol Phase State in Ammonia/Amines
457 Exchange Reactions, *Environ Sci Technol*, 47, 5755-5762, 10.1021/es4004685,
458 2013.
- 459 Cheng, C., Li, M., Chan, C. K., Tong, H., Chen, C., Chen, D., Wu, D., Li, L., Wu, C.,
460 Cheng, P., Gao, W., Huang, Z., Li, X., Zhang, Z., Fu, Z., Bi, Y., and Zhou, Z.:
461 Mixing state of oxalic acid containing particles in the rural area of Pearl River
462 Delta, China: implications for the formation mechanism of oxalic acid, *Atmos
463 Chem Phys*, 17, 9519-9533, 10.5194/acp-17-9519-2017, 2017.
- 464 Cheng, Y., Zheng, G., Wei, C., Mu, Q., Zheng, B., Wang, Z., Gao, M., Zhang, Q., He,
465 K., Carmichael, G., Pöschl, U., and Su, H.: Reactive nitrogen chemistry in
466 aerosol water as a source of sulfate during haze events in China, *Science
467 Advances*, 2, 10.1126/sciadv.1601530, 2016.



- 468 Chu, Y., and Chan, C. K.: Reactive Uptake of Dimethylamine by Ammonium Sulfate
469 and Ammonium Sulfate–Sucrose Mixed Particles, *J Phys Chem A*, 121, 206-215,
470 10.1021/acs.jpca.6b10692, 2016.
- 471 Chu, Y., and Chan, C. K.: Role of oleic acid coating in the heterogeneous uptake of
472 dimethylamine by ammonium sulfate particles, *Aerosol Sci Tech*, 51, 988-997,
473 10.1080/02786826.2017.1323072, 2017.
- 474 Chu, Y. X., Sauerwein, M., and Chan, C. K.: Hygroscopic and phase transition
475 properties of alkyl aminium sulfates at low relative humidities, *Phys Chem Chem*
476 *Phys*, 17, 19789-19796, 10.1039/c5cp02404h, 2015.
- 477 Day, D. A., Takahama, S., Gilardoni, S., and Russell, L. M.: Organic composition of
478 single and submicron particles in different regions of western North America and
479 the eastern Pacific during INTEX-B 2006, *Atmos Chem Phys*, 9, 5433-5446,
480 2009.
- 481 Denkenberger, K. A., Moffet, R. C., Holecek, J. C., Rebotier, T. P., and Prather, K. A.:
482 Real-time, single-particle measurements of oligomers in aged ambient aerosol
483 particles, *Environ Sci Technol*, 41, 5439-5446, 10.1021/es070329l, 2007.
- 484 Facchini, M. C., Decesari, S., Rinaldi, M., Carbone, C., Finessi, E., Mircea, M., Fuzzi,
485 S., Moretti, F., Tagliavini, E., Ceburnis, D., and O'Dowd, C. D.: Important
486 Source of Marine Secondary Organic Aerosol from Biogenic Amines, *Environ*
487 *Sci Technol*, 42, 9116-9121, 10.1021/es8018385, 2008.
- 488 Gard, E. E., Kleeman, M. J., Gross, D. S., Hughes, L. S., Allen, J. O., Morrical, B. D.,
489 Fergenson, D. P., Dienes, T., Gälli, M. E., and Johnson, R. J.: Direct observation
490 of heterogeneous chemistry in the atmosphere, *Science*, 279, 1184-1187, 1998.
- 491 Ge, X. L., Wexler, A. S., and Clegg, S. L.: Atmospheric amines - Part I. A review,
492 *Atmos Environ*, 45, 524-546, DOI 10.1016/j.atmosenv.2010.10.012, 2011a.
- 493 Ge, X. L., Wexler, A. S., and Clegg, S. L.: Atmospheric amines - Part II.
494 Thermodynamic properties and gas/particle partitioning, *Atmos Environ*, 45,
495 561-577, 10.1016/j.atmosenv.2010.10.013, 2011b.
- 496 Gilardoni, S., Liu, S., Takahama, S., Russell, L. M., Allan, J. D., Steinbrecher, R.,
497 Jimenez, J. L., De Carlo, P. F., Dunlea, E. J., and Baumgardner, D.:
498 Characterization of organic ambient aerosol during MIRAGE 2006 on three
499 platforms, *Atmos Chem Phys*, 9, 5417-5432, 2009.
- 500 Healy, R. M., Evans, G. J., Murphy, M., Sierau, B., Arndt, J., McGillicuddy, E.,
501 O'Connor, I. P., Sodeau, J. R., and Wenger, J. C.: Single-particle speciation of
502 alkylamines in ambient aerosol at five European sites, *Anal Bioanal Chem*, 407,
503 5899-5909, 10.1007/s00216-014-8092-1, 2015.
- 504 Huang, Y., Chen, H., Wang, L., Yang, X., and Chen, J.: Single particle analysis of
505 amines in ambient aerosol in Shanghai, *Environ Chem*, 9, 202-210,
506 10.1071/EN11145, 2012.
- 507 Jeong, C. H., McGuire, M. L., Godri, K. J., Slowik, J. G., Rehbein, P. J. G., and Evans,
508 G. J.: Quantification of aerosol chemical composition using continuous single
509 particle measurements, *Atmos Chem Phys*, 11, 7027-7044,
510 10.5194/acp-11-7027-2011, 2011.
- 511 Kurten, T., Loukonen, V., Vehkamäki, H., and Kulmala, M.: Amines are likely to



- 512 enhance neutral and ion-induced sulfuric acid-water nucleation in the atmosphere
513 more effectively than ammonia, *Atmos Chem Phys*, 8, 4095-4103, 2008.
- 514 Lee, D., and Wexler, A. S.: Atmospheric amines - Part III: Photochemistry and toxicity,
515 *Atmos Environ*, 71, 95-103, [10.1016/j.atmosenv.2013.01.058](https://doi.org/10.1016/j.atmosenv.2013.01.058), 2013.
- 516 Li, L., Huang, Z. X., Dong, J. G., Li, M., Gao, W., Nian, H. Q., Fu, Z., Zhang, G. H.,
517 Bi, X. H., Cheng, P., and Zhou, Z.: Real time bipolar time-of-flight mass
518 spectrometer for analyzing single aerosol particles, *Int J Mass Spectrom*, 303,
519 118-124, [10.1016/j.ijms.2011.01.017](https://doi.org/10.1016/j.ijms.2011.01.017), 2011.
- 520 Liu, S., Takahama, S., Russell, L. M., Gilardoni, S., and Baumgardner, D.:
521 Oxygenated organic functional groups and their sources in single and submicron
522 organic particles in MILAGRO 2006 campaign, *Atmos Chem Phys*, 9,
523 6849-6863, 2009.
- 524 Liu, Y., Han, C., Liu, C., Ma, J., Ma, Q., and He, H.: Differences in the reactivity of
525 ammonium salts with methylamine, *Atmos Chem Phys*, 12, 4855-4865, 2012.
- 526 Lloyd, J. A., Heaton, K. J., and Johnston, M. V.: Reactive uptake of trimethylamine
527 into ammonium nitrate particles, *J Phys Chem A*, 113, 4840-4843,
528 [10.1021/jp900634d](https://doi.org/10.1021/jp900634d), 2009.
- 529 Malloy, Q. G. J., Li, Q., Warren, B., Cocker III, D. R., Erupe, M. E., and Silva, P. J.:
530 Secondary organic aerosol formation from primary aliphatic amines with
531 NO₃ radical, *Atmos Chem Phys*, 9, 2051-2060,
532 [10.5194/acp-9-2051-2009](https://doi.org/10.5194/acp-9-2051-2009), 2009.
- 533 Moffet, R. C., de Foy, B., Molina, L. T., Molina, M. J., and Prather, K. A.:
534 Measurement of ambient aerosols in northern Mexico City by single particle
535 mass spectrometry, *Atmos Chem Phys*, 8, 4499-4516, [10.5194/acp-8-4499-2008](https://doi.org/10.5194/acp-8-4499-2008),
536 2008.
- 537 Murphy, S. M., Sorooshian, A., Kroll, J. H., Ng, N. L., Chhabra, P., Tong, C., Surratt,
538 J. D., Knipping, E., Flagan, R. C., and Seinfeld, J. H.: Secondary aerosol
539 formation from atmospheric reactions of aliphatic amines, *Atmos Chem Phys*, 7,
540 2313-2337, 2007.
- 541 Ngwabie, N. M., Schade, G. W., Custer, T. G., Linke, S., and Hinz, T.: Volatile organic
542 compound emission and other trace gases from selected animal buildings,
543 *Landbauforsch Volk*, 57, 273-284, 2007.
- 544 Noble, C. A., and Prather, K. A.: Real-time measurement of correlated size and
545 composition profiles of individual atmospheric aerosol particles, *Environ Sci
546 Technol*, 30, 2667-2680, 1996.
- 547 Place, P. F., Ziemba, L. D., and Griffin, R. J.: Observations of nucleation-mode
548 particle events and size distributions at a rural New England site, *Atmos Environ*,
549 44, 88-94, [10.1016/j.atmosenv.2009.09.030](https://doi.org/10.1016/j.atmosenv.2009.09.030), 2010.
- 550 Prather, K. A., Nordmeyer, T., and Salt, K.: Real-time characterization of individual
551 aerosol particles using time-of-flight mass spectrometry, *Anal Chem*, 66,
552 1403-1407, 1994.
- 553 Pratt, K., Murphy, S., Subramanian, R., DeMott, P., Kok, G., Campos, T., Rogers, D.,
554 Prenni, A., Heymsfield, A., and Seinfeld, J.: Flight-based chemical
555 characterization of biomass burning aerosols within two prescribed burn smoke



- 556 plumes, *Atmos Chem Phys*, 11, 12549-12565, 2011.
- 557 Pratt, K. A., Hatch, L. E., and Prather, K. A.: Seasonal Volatility Dependence of
558 Ambient Particle Phase Amines, *Environ Sci Technol*, 43, 5276-5281,
559 10.1021/es803189n, 2009.
- 560 Qiu, C., Wang, L., Lal, V., Khalizov, A. F., and Zhang, R.: Heterogeneous reactions of
561 alkylamines with ammonium sulfate and ammonium bisulfate, *Environ Sci
562 Technol*, 45, 4748-4755, 2011.
- 563 Rappert, S., and Muller, R.: Odor compounds in waste gas emissions from agricultural
564 operations and food industries, *Waste Manage*, 25, 887-907,
565 10.1016/j.wasman.2005.07.008, 2005.
- 566 Rehbein, P. J. G., Jeong, C. H., McGuire, M. L., Yao, X. H., Corbin, J. C., and Evans,
567 G. J.: Cloud and Fog Processing Enhanced Gas-to-Particle Partitioning of
568 Trimethylamine, *Environ Sci Technol*, 45, 4346-4352, 10.1021/es1042113, 2011.
- 569 Rogge, W. F., Hildemann, L. M., Mazurek, M. A., and Cass, G. R.: Sources of Fine
570 Organic Aerosol.6. Cigarette-Smoke in the Urban Atmosphere, *Environ Sci
571 Technol*, 28, 1375-1388, 10.1021/Es00056a030, 1994.
- 572 Russell, L. M., Takahama, S., Liu, S., Hawkins, L. N., Covert, D. S., Quinn, P. K., and
573 Bates, T. S.: Oxygenated fraction and mass of organic aerosol from direct
574 emission and atmospheric processing measured on the R/V Ronald Brown during
575 TEXAQS/GoMACCS 2006, *J Geophys Res-Atmos*, 114, 10.1029/2008jd011275,
576 2009.
- 577 Sauerwein, M., Clegg, S. L., and Chan, C. K.: Water Activities and Osmotic
578 Coefficients of Aqueous Solutions of Five Alkylammonium Sulfates and Their
579 Mixtures with H₂SO₄ at 25(o)C, *Aerosol Sci Tech*, 49, 566-579,
580 10.1080/02786826.2015.1043045, 2015.
- 581 Sauerwein, M., and Chan, C. K.: Heterogeneous uptake of ammonia and
582 dimethylamine into sulfuric and oxalic acid particles, *Atmos Chem Phys*, 17,
583 6323-6339, 10.5194/acp-17-6323-2017, 2017.
- 584 Silva, P. J., Erupe, M. E., Price, D., Elias, J., Malloy, Q. G. J., Li, Q., Warren, B., and
585 Cocker, D. R.: Trimethylamine as precursor to secondary organic aerosol
586 formation via nitrate radical reaction in the atmosphere, *Environ Sci Technol*, 42,
587 4689-4696, Doi 10.1021/Es703016v, 2008.
- 588 Sorooshian, A., Ng, N. L., Chan, A. W. H., Feingold, G., Flagan, R. C., and Seinfeld, J.
589 H.: Particulate organic acids and overall water-soluble aerosol composition
590 measurements from the 2006 Gulf of Mexico Atmospheric Composition and
591 Climate Study (GoMACCS), *J Geophys Res-Atmos*, 112, 10.1029/2007jd008537,
592 2007.
- 593 Sorooshian, A., Murphy, S. N., Hersey, S., Gates, H., Padro, L. T., Nenes, A., Brechtel,
594 F. J., Jonsson, H., Flagan, R. C., and Seinfeld, J. H.: Comprehensive airborne
595 characterization of aerosol from a major bovine source, *Atmos Chem Phys*, 8,
596 5489-5520, 2008.
- 597 Wang, G., Zhang, R., Gomez, M. E., Yang, L., Levy Zamora, M., Hu, M., Lin, Y.,
598 Peng, J., Guo, S., Meng, J., Li, J., Cheng, C., Hu, T., Ren, Y., Wang, Y., Gao, J.,
599 Cao, J., An, Z., Zhou, W., Li, G., Wang, J., Tian, P., Marrero-Ortiz, W., Secretst, J.,



600 Du, Z., Zheng, J., Shang, D., Zeng, L., Shao, M., Wang, W., Huang, Y., Wang, Y.,
601 Zhu, Y., Li, Y., Hu, J., Pan, B., Cai, L., Cheng, Y., Ji, Y., Zhang, F., Rosenfeld, D.,
602 Liss, P. S., Duce, R. A., Kolb, C. E., and Molina, M. J.: Persistent sulfate
603 formation from London Fog to Chinese haze, *P Natl Acad Sci USA*, 113,
604 13630-13635, 10.1073/pnas.1616540113, 2016.

605 Wang, L., Khalizov, A. F., Zheng, J., Xu, W., Ma, Y., Lal, V., and Zhang, R. Y.:
606 Atmospheric nanoparticles formed from heterogeneous reactions of organics, *Nat*
607 *Geosci*, 3, 238-242, 10.1038/NGEO778, 2010.

608 Williams, B. J., Goldstein, A. H., Kreisberg, N. M., Hering, S. V., Worsnop, D. R.,
609 Ulbrich, I. M., Docherty, K. S., and Jimenez, J. L.: Major components of
610 atmospheric organic aerosol in southern California as determined by hourly
611 measurements of source marker compounds, *Atmos Chem Phys*, 10,
612 11577-11603, 10.5194/acp-10-11577-2010, 2010.

613 Zhang, G., Bi, X., Chan, L. Y., Li, L., Wang, X., Feng, J., Sheng, G., Fu, J., Li, M.,
614 and Zhou, Z.: Enhanced trimethylamine-containing particles during fog events
615 detected by single particle aerosol mass spectrometry in urban Guangzhou, China,
616 *Atmos Environ*, 55, 121-126, 2012.

617 Zhang, G., Bi, X., Li, L., Chan, L. Y., Li, M., Wang, X., Sheng, G., Fu, J., and Zhou,
618 Z.: Mixing state of individual submicron carbon-containing particles during
619 spring and fall seasons in urban Guangzhou, China: a case study, *Atmos Chem*
620 *Phys*, 13, 4723-4735, 2013.

621
622
623
624
625
626
627
628
629
630
631
632
633
634
635
636
637
638
639
640
641
642
643



644 **Tables and Figures**

645

646 **Table list:**

647 Table 1. Seasonal distributions of major types of amine-containing particles in
648 summer and winter in the PRD, China.

649

650

651 **Figure captions:**

652 Figure 1. Seasonal distributions of amine-containing particle number concentrations
653 associated with wind direction and wind speed in (left) summer and (right) winter.

654

655 Figure 2. Temporal variations in amine-containing particles, relative humidity (RH),
656 temperature (T), wind speed (WS), wind direction, and three types of amine particles
657 in Heshan, China during the entire sampling periods. Abbreviations of major particle
658 types: elemental and organic carbon (ECOC); biomass burning (BB).

659

660 Figure 3. Diurnal variations in amine-containing particle number concentrations in
661 summer and winter in Heshan.

662

663 Figure 4. Average ion mass spectra of ECOC, BB, and nitrate-rich amine-containing
664 particles in (a) summer and (b) winter.

665

666 Figure 5. Size distributions of the three types of amine-containing particles in (a)
667 summer and (b) winter.

668

669 Figure 6. Mixing states of ammonium, nitrate, and sulfate in the three types of
670 amine-containing particles during summer and winter.

671

672 Figure 7. Temporal variations in the peak areas of amines, ammonium, and the sum of
673 sulfate and nitrate in ECOC amine-containing particles during summer and winter.
674 The relative acidity ratio (R_a), which was calculated as the ratio of the total sulfate and
675 nitrate peak areas to the ammonium peak area, is plotted as $\log(R_a)$.

676

677

678

679

680

681

682

683



684 **Table:**

685

686

687

688

Table 1. Seasonal distributions of major types of amine-containing particles
in summer and winter in the PRD, China.

Particle type	Summer (18/7-1/8, 2014)		Winter (27/1-8/2, 2015)	
	Count	Percentage (%)	Count	Percentage (%)
ECOC	44576	67.2	52864	74.8
BB	8546	12.9	11499	16.3
Nitrate-rich	8879	13.4	2597	3.7
Unclassified	4330	6.5	3688	5.2

Abbreviations of major particle types: elemental and organic carbon (ECOC), biomass burning (BB), nitrate-rich.

689

690

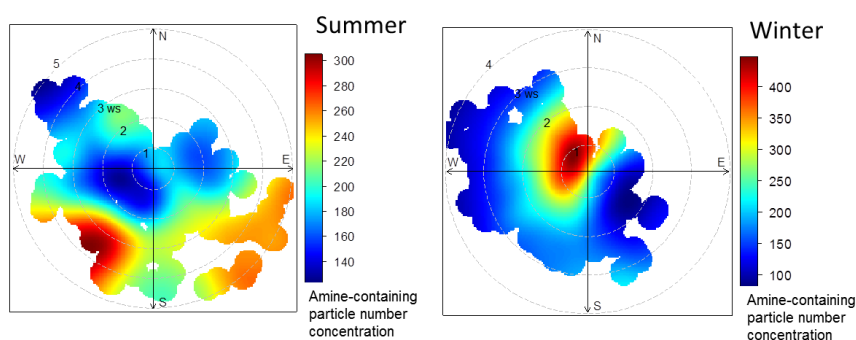
691

692

693

694 **Figures:**

695



696

697

698 Figure 1. Seasonal distributions of amine-containing particle number concentrations
699 associated with wind direction and wind speed in (left) summer and (right) winter.

700

701

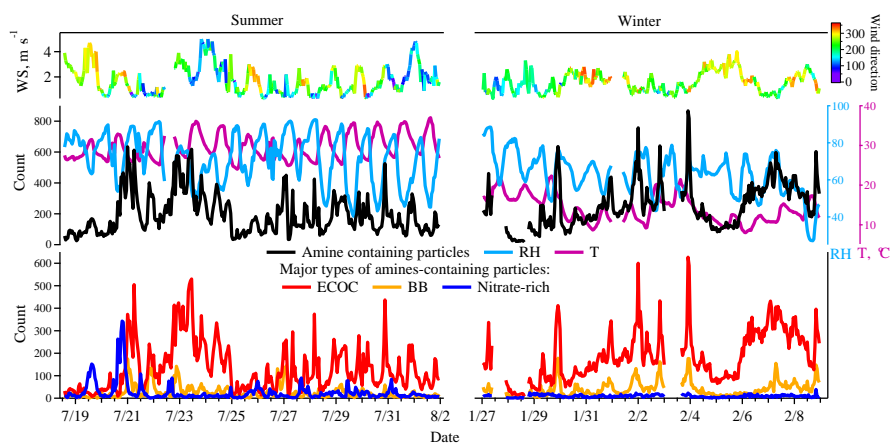
702

703

704



705



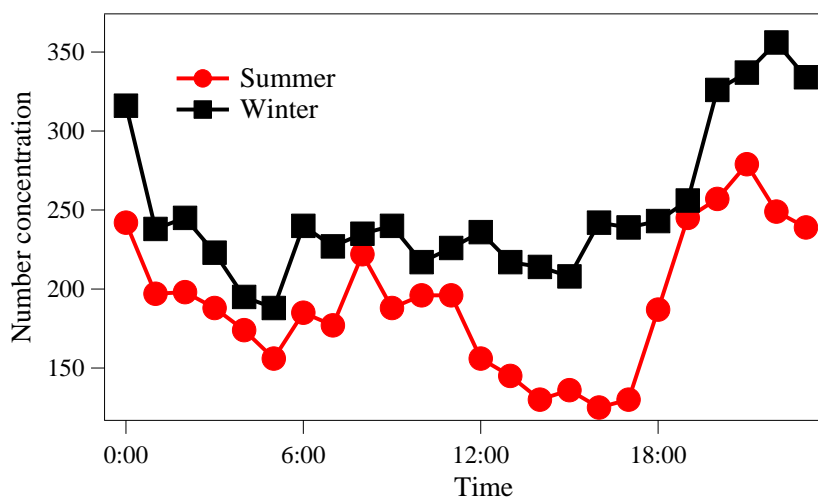
706

707 Figure 2. Temporal variations in amine-containing particles, relative humidity (RH),
708 temperature (T), wind speed (WS), wind direction, and three types of amine particles
709 in Heshan, China during the entire sampling periods. Abbreviations of major particle
710 types: elemental and organic carbon (ECOC); biomass burning (BB).

711

712

713



714

715 Figure 3. Diurnal variations in amine-containing particle number concentrations in
716 summer and winter in Heshan.

717

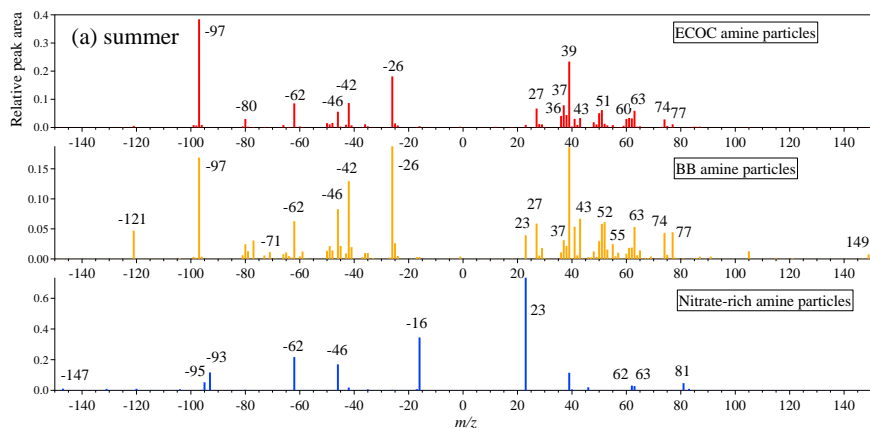
718

719

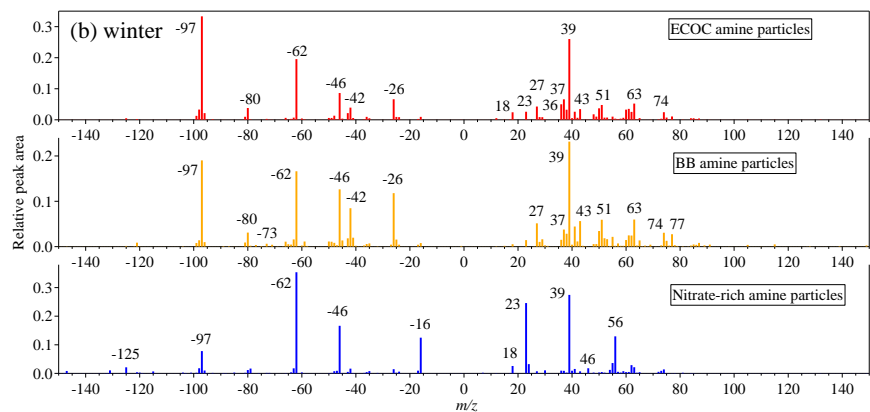
720



721
722



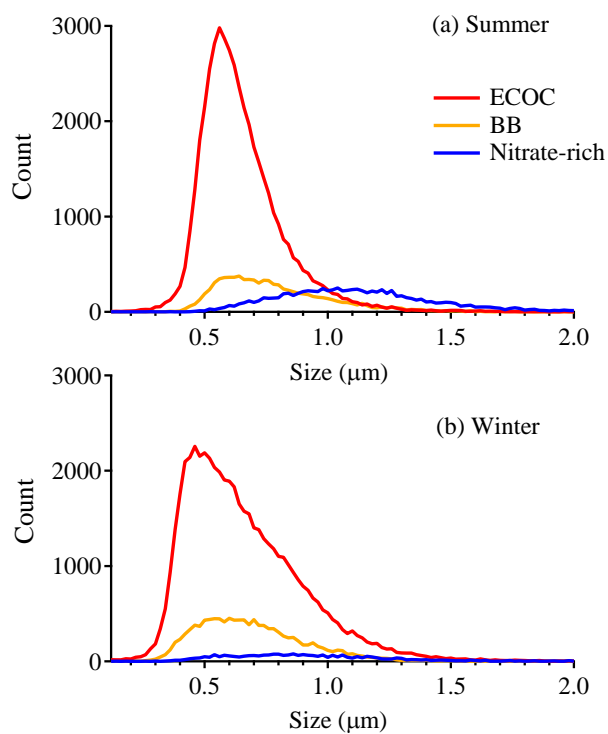
723



724

725 Figure 4. Average ion mass spectra of ECOC, BB, and nitrate-rich amine-containing
726 particles in (a) summer and (b) winter.

727
728
729
730
731
732
733
734
735
736
737
738
739
740



741

742 Figure 5. Size distributions of the three types of amine-containing particles in (a)
743 summer and (b) winter.

744

745

746

747

748

749

750

751

752

753

754

755

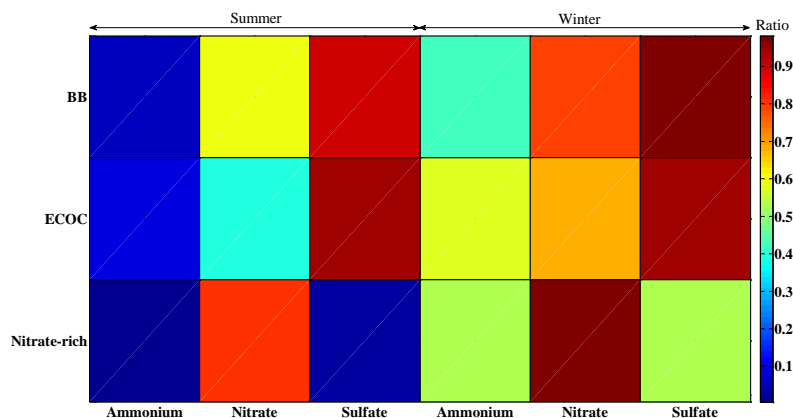
756

757

758

759

760



761

762 Figure 6. Mixing states of ammonium, nitrate, and sulfate in the three types of
 763 amine-containing particles during summer and winter.

764

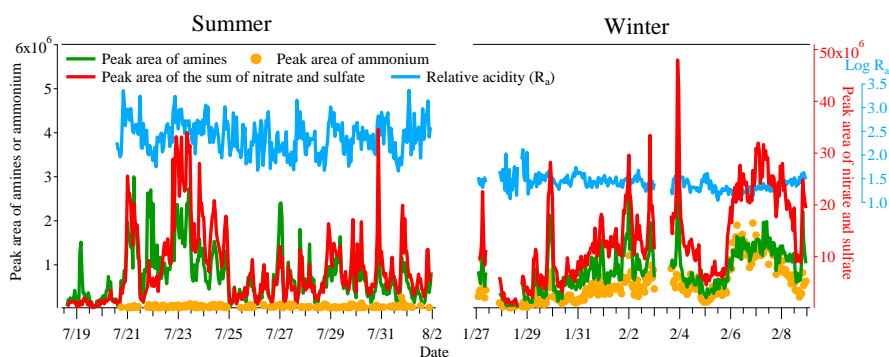
765

766

767

768

769



770

771 Figure 7. Temporal variations in the peak areas of amines, ammonium, and the sum of
 772 sulfate and nitrate in ECOC amine-containing particles during summer and winter.
 773 The relative acidity ratio (R_a), which was calculated as the ratio of the total sulfate and
 774 nitrate peak areas to the ammonium peak area, is plotted as $\log(R_a)$.

775

776